Intracellular Release of Endocytosed Nanoparticles Upon a Change of Ligand–Receptor Interaction

Robert Vácha,[†,*] Francisco J. Martinez-Veracoechea,[‡] and Daan Frenkel[‡]

[†]National Centre for Biomolecular Research, Faculty of Science and CEITEC—Central European Institute of Technology, Masaryk University, Kamenice 5, 625 00 Brno-Bohunice, Czech Republic, and and [‡]Department of Chemistry, University of Cambridge, Lensfield Road, Cambridge, CB2 1EW, United Kingdom

ABSTRACT During passive endocytosis, nanosized particles are initially encapsulated by a membrane separating it from the cytosol. Yet, in many applications the nanoparticles need to be in direct contact with the cytosol in order to be active. We report a simulation study that elucidates the physical mechanisms by which such nanoparticles can shed their bilayer coating. We find that nanoparticle release can be readily achieved by a pH-induced lowering of the attraction between nanoparticle and membrane only if the nanoparticle is either very small or nonspherical. Interestingly, we find that in the case of large spherical nanoparticles, the reduction of attraction needs to be accompanied by exerting an additional tension on the membrane (*e.g., via* nanoparticle expansion) to achieve release. We expect these findings will contribute to the rational design of drug delivery strategies *via* nanoparticles.

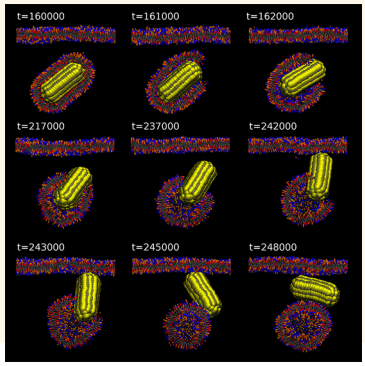

KEYWORDS: cytosol release · late endosome · ligand–receptor interaction · phospholipid membrane · nanoparticle shape · molecular dynamics

Current efforts in nanomedicine focus on treatments at the individual cell level such that affected cells can be treated without damaging the healthy ones, thus reducing side effects.[1−3] Such an approach requires efficient delivery strategies that allow drugs to be taken up by, and released in, the target cells with high specificity. One promising strategy to carry drugs is the usage of multivalent nanoparticles, liposomes, or similar particles, as they can be designed to adhere selectively to surfaces that display a given type of receptor.[1,4,5] When the attraction between the ligands on a nanoparticle and the receptors on the cell surface is strong enough, the nanoparticle can be fully internalized through passive endocytosis—a spontaneous (thermodynamically driven) process that does not require the consumption of ATP.[6−8] When a nanoparticle is fully internalized in a cell by endocytosis, it becomes encapsulated by a membrane or endosome, and is therefore still separated from the cytosol. In many applications,[9] the nanoparticle or its components need to be released into the cytosol in order to become active. This is particularly crucial in the case of siRNA therapy where early release is necessary to avoid degradation in the lyzosome.[10]

The release can be triggered by a change of conditions in the endosome such as a slight pH change.[11] Naturally, this change of conditions can influence the receptor–ligand interaction, for example by diminishing its strength.[12] Because of the multivalent nature of the nanoparticle–membrane interactions, a slight decrease in the interaction strength can lead to significant changes in membrane–nanoparticle wrapping, and as we show in this study, it can even cause the full release of the nanoparticle from the endosome into the cytoplasm.

Relatively little is known about the minimum ingredients necessary for the full release of nanoparticles that have undergone passive endocytosis. In this paper, we investigate the release mechanism of such systems by modifying the strength of the interaction between the nanoparticle's ligands and membrane receptors. In particular, we consider the effect of the size and shape of the nanoparticle and of the degree of tension in the encapsulating bilayer. Using a coarse grained description and comparison to an elastic model allows us to study a generic physical mechanism of nanoparticle escape.

* Address correspondence to robert.vacha@mail.muni.cz, robertvacha@gmail.com.

Received for review August 3, 2012 and accepted November 2, 2012.

Published online November 13, 2012
10.1021/nn303508c

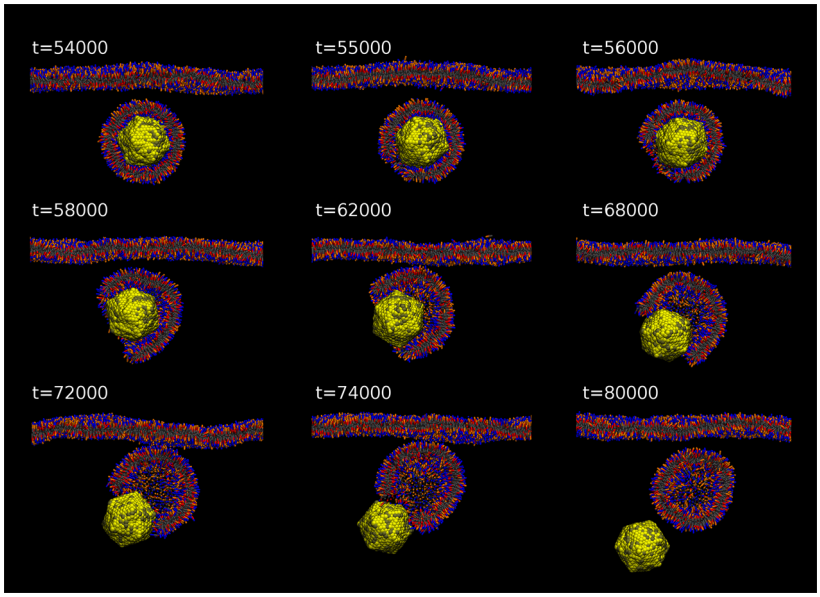

Figure 1. Several representative snapshots of a MD trajectory where the nanoparticle is released from the enclosing vesicle. The initial configuration was taken from the end of an endocytosis simulation (t = 54000) but the strength of the ligand−receptor interaction was changed to 0 kT, mimicking a change of the interactions due to a different endosomal environment. A pore opens in the encapsulating membrane upon the loss of attraction to the nanoparticle. The pore then expands and the nanoparticle is released. Consequently, the vesicle closes again (t = 80000). The snapshots display a cut through the membrane at the particle position, where the surface is composed of ligands homogeneously distributed on the surface. Color coding: (nanoparticle) yellow beads are ligands and gray beads are purely repulsive; (membrane) blue beads are membrane receptors, orange are headgroups, and gray and red are tail beads.

We have employed Molecular Dynamics (MD) simulations using an implicit-solvent coarse-grained model, in which the phospholipid molecules of the membrane are represented by a three-bead model.[13] The first bead (hydrophilic headgroup) is purely repulsive, while the other two beads, representing hydrophobic tails, attract each other. Nanoparticles of different sizes and shapes are constructed from beads of similar size as those of the phospholipids (see Methods). About half of the nanoparticle surface beads (ligands) are selectively attractive to membrane "receptors" that differ from the phospholipids by the fact that the "head groups" selectively attract the ligands of the nanoparticles. In this study, 50% of the membrane lipids can act as receptors. More details about the model can be found in the Methods section and in ref 6, which focuses on the early stages of endocytosis.

RESULTS AND DISCUSSION

A typical release event of a spherical nanoparticle with diameter 9.6 nm is depicted in Figure 1. We show the snapshots from the time when the ligand−receptor attraction was changed instantaneously from −5 to 0 kT (mimicking the effect of pH change). The change of interaction is followed by a rapid pore opening in the encapsulating membrane. Once the pore is large enough, the nanoparticle is released. After the complete release of the nanoparticle the membrane pore closes.

A similar process was observed for spherocylinders, that is, cylindrical particles with hemispherical caps at the ends, with aspect ratios of 2.0 and 1.0 (see Figure 2). Importantly, in the case of spherocylinders the pore opened at the end of the spherocylinder, which is the place with the highest mean curvature. The whole process of release was faster for spheres than for spherocylinders with the same diameter, which is expected as spherocylinders are larger and consequently diffuse more slowly.

As the membrane/encapsulated-nanoparticle complex is stabilized by the ligand−receptor attraction, we expect that nanoparticles will have the potential to be released once the strength of the attraction falls below a given critical value. However, even when the encapsulated state of the nanoparticle becomes thermodynamically less stable than the released state, kinetic considerations will determine whether or not we can observe the release of the nanoparticle within the time scale of our simulations. The free-energy barrier for release determines whether or not we will be able to observe the release process on the time scale of our simulations. In fact, for both spherical and spherocylindrical nanoparticles, we observe spontaneous particle release whenever the ligand−receptor attraction energy is decreased below a fairly sharp (geometry-dependent) threshold. This is shown in Table 1. However, the complex interplay between thermodynamic and kinetic factors makes it difficult to predict the dependence of this threshold value on the size and shape of the nanoparticles. For instance, spontaneous release was observed both for a sphere (D = 9.6 nm)

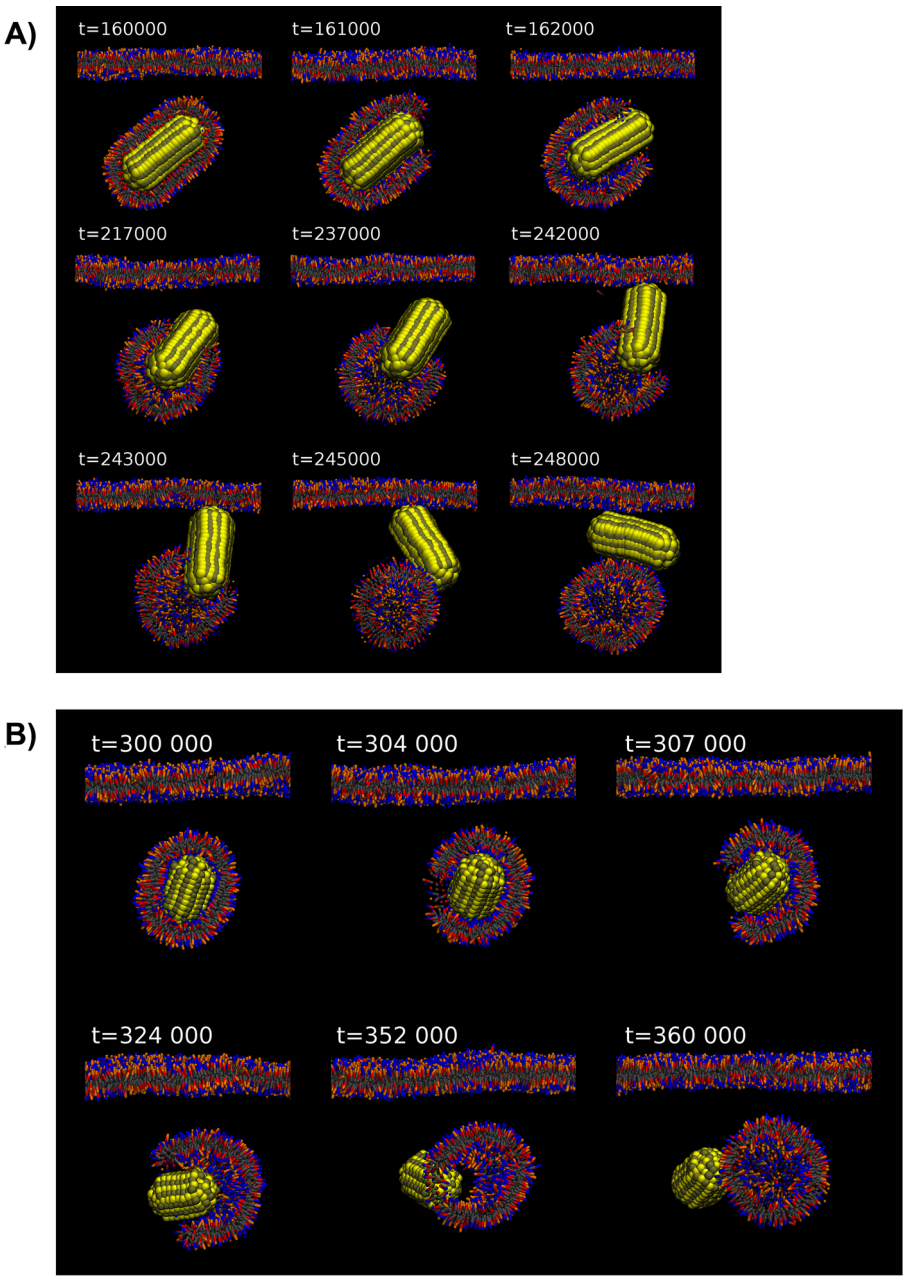

Figure 2. Several representative snapshots of a MD trajectory where nanoparticles of spherocylindrical shape are released from an enclosed vesicle. Two aspect ratios 2.0 (A) and 1.0 (B) were studied. The initial configuration was taken from the end of an endocytosis simulation and the strength of ligand−receptor interaction was modified from −5.0 to 0 kT. A pore opens in the encapsulating membrane upon the loss of attraction to the nanoparticle and the nanoparticle diffuses through the pore outward. After the nanoparticle is released the vesicle closes again. The snapshots display a cut through the membrane at the middle of the vesicle. Color coding: same as in Figure 1.

TABLE 1. Results of the Simulation with Membrane Encapsulated Nanoparticle after Receptor-Mediated Endocytosis, Where the Ligand-Receptor Interaction Was Made Weaker (from Initial −5.0 kT in All Cases Except for the Small Sphere, Where the Initial Strength Was −8.0 kT)

residual binding strength (kT)	spherocylinder aspect ratio 2:1	spherocylinder aspect ratio 1:1	sphere diameter 9.6 nm	sphere diameter 5.2 nm
−2.0	encapsulated	encapsulated	encapsulated	encapsulated
−1.5	encapsulated	exposed tip	encapsulated	encapsulated
−1.0	encapsulated	released	released	released
−0.5	released	released	released	released
−0.0	released	released	released	released

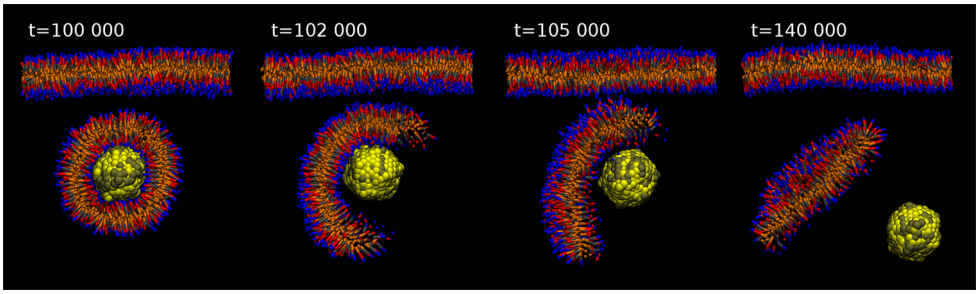

Figure 3. Snapshots from our MD simulation with a small nanoparticle, where the membrane ended as a flat disk after the nanoparticle was released. The initial configuration started from a fully encapsulated nanoparticle after receptor−ligand mediated, passive endocytosis. At the start (t = 100000) the strength of the ligand−receptor interaction changed from −8.0 to 0 kT. This resulted in a fast opening of a membrane pore, which expanded as the membrane flattened (t = 105000). At the end of the process, the nanoparticle was fully released and the membrane formed a flat disk. The snapshots display a cut through the membrane at the particle position; 80% of the particle's surface beads are ligands. Color coding: same as in Figure 1.

and a for spherocylinder of similar diameter (D = 9 nm, L = 9 nm) and with aspect ratio 1.0 when the ligand−receptor interaction strength dropped to about −1.0 kT, while a spherocylinder with an aspect ratio of 2 (D = 9 nm, L = 18 nm) was only released at a slightly weaker ligand−receptor interaction (−0.5 kT).

The physics underlying the release process can be understood in terms of the elastic theory that describes the membrane as a thin, flexible (and stretchable) sheet. The free energy of local deformations can be estimated using the expression proposed by Helfrich,[14] which for any sphere simplifies to a constant: $8\pi\kappa + 4\pi\kappa_G$. Here κ and κ_G are, respectively, the bending rigidities associated with the mean and Gaussian curvatures. While the value of the bending rigidity has been reliably measured to be about 20 kT,[15,16] the bending rigidity associated with Gaussian curvature is more difficult to obtain.[17,18] Recent estimates suggest values of around -0.8κ.[19,20] Thus, the total bending free energy of a symmetric bilayer encapsulating a sphere of any size can be approximated to be around 300 kT. Using a similar procedure one can evaluate the bending energy for spherocylindrical shape.[6]

To achieve encapsulation, the membrane bending free energy must be compensated by the attraction between membrane receptors and nanoparticle ligands. When the stabilizing receptor−ligand interaction is decreased, the equilibrium state of the surrounding membrane will be determined by a competition among several factors such as the bending energy, the internal pressure inside the bilayer shell, the line tension of the edge of an incipient pore, and the translational entropy of both the vesicle and the nanoparticle. While minimization of the bending energy would favor the formation of a flat disk of membrane (zero curvature), the line tension will favor the formation of a vesicle. The line tension quantifies the penalty associated with the exposure of a membrane edge and has been measured to be between 6.5 and 30 pN.[21−24]

Thus, in the case of a very small vesicle (surrounding a small nanoparticle), reduction of the attractive interactions between membrane and particle can result in the formation of a flat membrane "disk". Indeed, this is precisely what we observe in the case of a small nanoparticle with diameter about 5.2 nm (see Figure 3). If we employ the above numbers for bending rigidity and line tension in eq 2 and eq 5 we can see that the bending energy of a sphere is enough to expose 80 nm of the membrane edge. In other words this means that vesicles with a diameter smaller than 12 nm would be thermodynamically stable as a flat disk. This size is likely to be an upper bound, since we have observed in the simulations that lipids can quickly exchange between the leaflets when a pore is opened *via* translocation and thus the bending energy can be reduced. Repeated simulations with a nanoparticle of diameter 9.7 nm resulted, after the release, in both membrane geometries: disk and vesicle. This result agrees well with previous simulations that found that membrane discs of diameter from 9 to 20 nm coexisted with membrane vesicles.[25]

For membranes encapsulating larger nanoparticles, the penalty of having a free edge becomes too large. Hence, the most stable state of the membrane is a closed spherical vesicle. Therefore, when the nanoparticle is elongated, as in the case of spherocylinders, its release will have a strong thermodynamic drive. If there is some residual ligand−receptor attraction, there will be a competition between the bending energy and the attraction. As a result, the final membrane shape and the release process will depend on the precise value of this residual energy (see Table 1).

In the case of large, spherical particles, the free energy barrier for release becomes very high, while the driving force for release becomes dominated by the (usually small) gain in translational entropy. Under these conditions, spontaneous release becomes very slow and, indeed a simulation of a large (diameter of 14 nm), encapsulated spherical particle did not show release in the course of a very long simulation.

However, the rate of release of large nanoparticles can be increased if the encapsulating membrane is

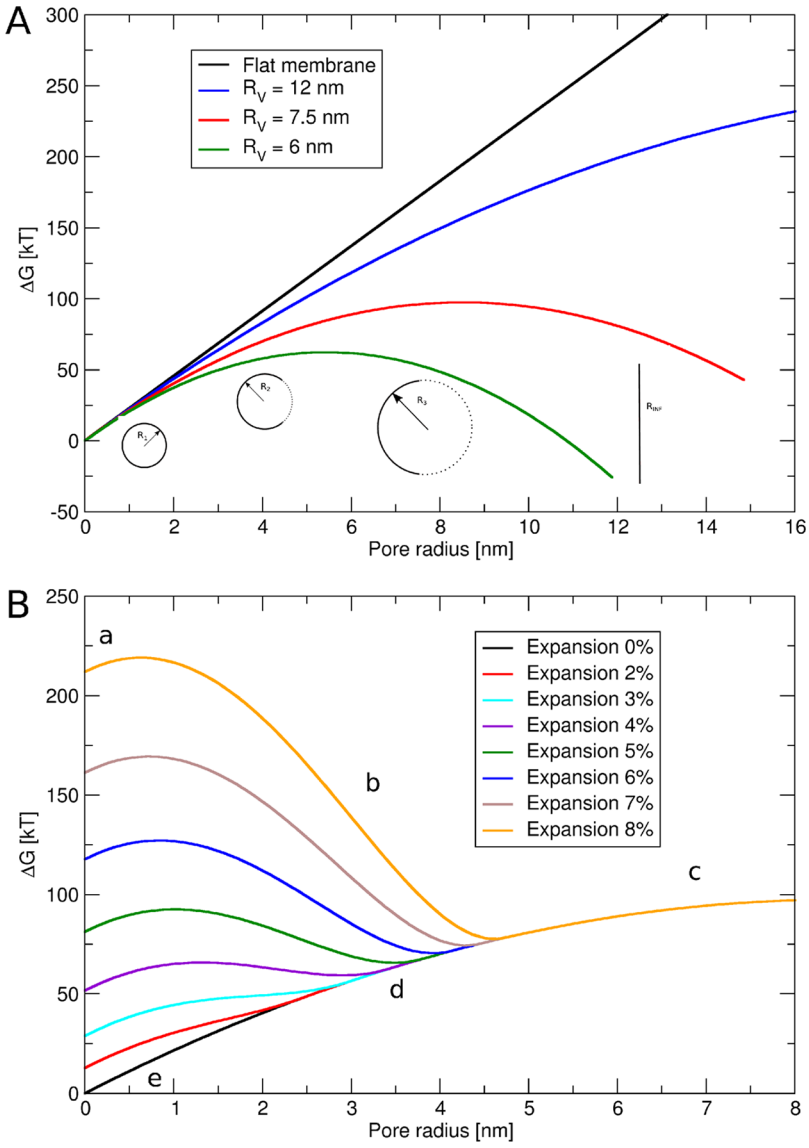

Figure 4. The free energy profiles as a function of pore size evaluated from an elastic model (see Methods section). (A) Results for tensionless vesicles of various sizes in comparison with a flat membrane; (B) changes of the free energy profiles when the nanoparticle expands and pressurizes the vesicle. The nanoparticle radius was 5.0 nm before the expansion and the vesicle was initially at zero tension. Letters a–e follow the free energy path of release process of the nanoparticle after the radius expansion of 8%.

stretched. Stretching of the encapsulating membrane may be achieved in several ways, but the effects are always the same. Here we consider the situation where the nanoparticle is slightly compressed during encapsulation, due to strong receptor–ligand interactions. Once the interaction is switched off, the membrane is in a state of stress. As an example, we consider the case where the radius of the encapsulated nanoparticles is initially 4% less than that of released nanoparticle. Once the ligand–receptor interaction is switched off the nanoparticle tends to re-expand, thereby stretching the encapsulating membrane. This stretching facilitates the release of the nanoparticle, as can be seen in Figure 1. Note that the membrane vesicle reverts to a spherical shell after releasing its cargo, thus confirming that it is the surface stretching rather than the membrane bending that drives the release.

We note that enhancement of cargo release due to the internal pressure on the membrane has been exploited in experimental applications of gene delivery: in this case, the nanoparticles were made of polyethyleneimine that increases its charge upon the decrease of pH, and thereby expands. It was found that this process facilitates endosomal delivery.[10] Interestingly, virus capsids can expand by up to 10% upon a change of pH[26,27] suggesting that viruses may also exploit this mechanism to aid their release.

The rate of the release process is limited by the formation of a pore in the vesicle that will allow the nanoparticle to escape. Pore formation is a rare event,

as it involves an appreciable free energy cost. We have estimated the height of this free-energy barrier using a Helfrich-like model, where we assume that the shape of the remainder of the vesicle remains spherical during pore formation (see Methods and Figure 4A). Our results are in agreement with the computer simulations of Shinoda, who used computer simulations to compute the free-energy cost of pore-opening in a vesicle.[28] We conclude that the free-energy cost of the spontaneous formation of a pore of radius larger than 5 nm in a tension-free vesicle is so high that the process is effectively forbidden.

However, if the membrane is under tension, the release barrier can be greatly reduced as opening a membrane pore is a more favorable process than stretching the membrane for more than 5%.[29,30] From the elastic model (see Methods), we can calculate the energy barrier associated with pore opening when the vesicle is under tension due to the internal pressure of the nanoparticle (see Figure 4). As can be seen in this figure, even a slight increase in the radius of the encapsulated particle strongly increases the free energy of the encapsulated state. As a consequence, the free-energy barrier for pore formation is decreased and the rate of the nanoparticle release is strongly enhanced.

To validate our simple analytical model, we have used MD simulations to compute the free-energy cost associated with the expansion of an encapsulated nanoparticle. The free energy cost associated with the expansion of an encapsulated sphere from a radius of 5.0 to 5.2 nm, is 40 kT. This is roughly in agreement with the 50 kT calculated from the elastic model (4% expansion). When we expanded the internalized particle's radius from 5.0 to 5.4 nm, a membrane pore spontaneously opened and the particle was released. The observed release process is in agreement with the data from the elastic model Figure 4B (8% expansion). In Figure 4B, we can follow the most favorable trajectory for release: (a) at the beginning the expanded nanoparticle causes tension on the enclosed vesicle as no pore is present (*i.e.*, pore radius = 0). (b) After crossing a small free energy barrier a pore of finite size is opened and the free energy decreases. (c) If the pore radius is large enough (roughly equal to the radius of the nanoparticle) the particle can be released. Once the vesicle is empty, it becomes favorable to (d) decrease the pore size until (e) the vesicle is closed.

CONCLUSIONS

In summary: we have used MD simulations to study the cytosol release of particles that have been internalized *via* passive endocytosis. At our coarse grained level of description our particles can represent either artificial nanoparticles or simplified proto-typical virus capsids. Typically, we find that the release process can occur spontaneously if the strength of attraction between nanoparticle ligands and the membrane receptors is lowered sufficiently. A significant thermodynamic driving force for release exists when the strength of attraction is no longer dominant and the endosome is either (1) small enough that it prefers a flat disk conformation or (2) sufficiently deformed from its equilibrium state. This deformation can be provided by the elongated shape of the encapsulated nanoparticle or by a pressure exerted by the nanoparticle on the membrane. This internal pressure can be achieved by a judicious choice of materials, which would expand in the late endosome, or by normal expansion of deformable nanoparticles that have been compressed during the initial phase of the uptake process. Since there is no elastic driving force for the release of encapsulated nanoparticles that are rigid, large, and spherical, we do not observe their release during any of our simulations. Nevertheless, it is possible that such particles' release will be driven by other factors (*e.g.*, membrane fluctuations and translational entropy gains) albeit on much longer time scales than the ones considered here.

The insights that the present work provides in the role of membrane deformation on nanoparticle release should facilitate the rational design drug-delivery strategies that are based on passive endocytosis of a nanosized cargo.

METHODS

Simulation Details. The simulations details are explained thoroughly in our previous study,[6] therefore here we describe them only briefly. For the phospholipids we employed the recently developed implicit solvent coarse-grained model of Cooke and Deserno, which has been shown to reproduce the experimental elastic properties of membranes such as the compressibility, the bending modulus, pore line tension, Gaussian modulus, and elasticity of membrane tubes.[31,19] Phospholipids are represented by a chain of three beads. The first bead is purely repulsive and represents the hydrophilic headgroup. The last two beads represent the hydrophobic tail and are attractive to other tail beads. The surface of the nanoparticle was made of similar repulsive beads as the lipid headgroups, but some of the beads (ligands) were made attractive to 50% of the lipid headgroups (representing membrane receptors). In this work, the number of ligands per particle was varied between 50 and 80% of the nanoparticle's surface beads; 50% of ligands was used for the larger sphere (Figure 1) and 80% was used for the smaller sphere (Figure 3). For simplicity, the attractive potential was chosen to be of the same form as that between the hydrophobic tails; however, the range of attraction was shorter (about 30% of the diameter) and the depth of the attractive well varied as a control parameter of the ligand−receptor binding strength. Icosahedral virus-like nanoparticles were constructed as a hollow interconnected shell, which was filled with larger soft spheres in order to keep the spherical shape by inner pressure. As such, the particle is slightly deformable with preferred roughly spherical shape. The smaller nanoparticle was constructed from 122 beads forming a shell and 72 beads inside,

while the larger nanoparticle was constructed using 792 beads for the shell and 252 beads inside. Spherocylinders were built out of the same beads with 61 beads in the cross-section. For more details on construction of the nanoparticles see ref 6. We have also studied nondeformable nanoparticles made of a single hard bead to study the effects of deformability.

All our simulations were carried out using the Molecular Dynamics package ESPRESSO.[32] The simulated systems consisted of 8000 lipids placed in a rectangular cell with fixed *z*-direction and varying *xy*-plane. Employing periodic boundary conditions this yields an infinite membrane bilayer in the *xy*-plane, which was kept at zero pressure. The temperature of the system was kept by the Langevine thermostat at 1.0 kT resulting in a membrane in the liquid fluid phase. The time step was chosen as in the original lipid study[13] at 0.01τ and the total time of simulations was on the order of $10^5\tau$.

The unit of time was estimated *via* lipid diffusion to be $\tau = 10$ ns; however, this is just a rough approximation since we treat the solvent implicitly. Lengths are measured in units of a lipid bead diameter (1σ), which we roughly estimated to be about 1 nm by comparison of the simulated membrane thickness (i.e., 5σ) to its experimental value (about 5 nm). Note that because of the comparison with the rigid nanoparticle made of a single bead, we have measured the nanoparticle's radius from the center to the surface (not by the distance up to the surface beads as in our previous study[6]).

The free energy associated with isotropic expansion of a hard sphere encapsulated by a vesicle was calculated *via* Bennett's method.[33] The energy differences were obtained using two simulations with particles of radius 5.0 and 5.2 nm and employing virtual moves of particle expansion and contraction.

Release Barrier from Elastic Model. From an elastic point of view a membrane can be approximated as an infinitely thin sheet of flexible material. The free energy of membrane deformation can be expressed through the Helfrich equation:[14]

$$G_{\text{deformation}} = G_{\text{bend}} + G_{\text{stretch}} = \int \frac{\kappa}{2}\left(\frac{1}{R_1}+\frac{1}{R_2}\right)^2 + \kappa_G \frac{1}{R_1 R_2}\,dA + \frac{1}{2}K_s\frac{(A-A_0)^2}{A_0} \quad (1)$$

where R_1 and R_2 are the local principal curvatures of the membrane surface, and κ and κ_G are the bending rigidities of the membrane, associated with the mean and Gaussian curvature. K_s is a stretching constant and A_0 is the tensionless area.

Before the release can happen, there has to be a membrane pore opened, through which the enclosed nanoparticle can escape. The free energy cost of opening such a pore is associated with the unfavorable membrane edge exposed to water. In continuum theory this is expressed in terms of line tension γ. The free energy of a pore is then

$$G_{\text{pore}} = \int \gamma\, dl \quad (2)$$

The total free energy of a membrane vesicle with a pore is given by

$$G_{\text{TOT}} = \int \frac{\kappa}{2}\left(\frac{1}{R_1}+\frac{1}{R_2}\right)^2 + \kappa_G \frac{1}{R_1 R_2}\,dA + \int \gamma\, dl + \frac{1}{2}K_s\frac{(A-A_0)^2}{A_0} \quad (3)$$

If we assume that the vesicle has the shape of a spherical cap, the formula simplifies to

$$G_{\text{TOT}} = (2\kappa+\kappa_G)\frac{A}{R^2} + 2\pi\gamma x + \frac{1}{2}K_s\frac{(A-A_0)^2}{A_0} \quad (4)$$

where x is a pore radius and R is the radius of the vesicle. For a closed vesicle of spherical geometry in equilibrium this simplifies to

$$G_{\text{sphere}} = 4\pi(2\kappa+\kappa_G) \quad (5)$$

The free energy difference between the closed vesicle with radius R_0 and an opened vesicle with radius R and pore radius x is

$$\Delta G = 2\pi\gamma x + 2\pi(2\kappa+\kappa_G)\left(\sqrt{1-\frac{x^2}{R^2}}-1\right) + \frac{\pi K_s}{2{R_0}^2}\left[R^2\left(1+\sqrt{1-\frac{x^2}{R^2}}\right) - 2{R_0}^2\right]^2 \quad (6)$$

The free energy profiles from this equation are presented in Figure 5. For each pore size we found the value of R that minimizes the total free energy, with the lower limit set by the radius of the enclosed nanoparticle. Note that for a more direct comparison with the simulations, we have taken into account the 5 nm width of the membrane, and the size of the vesicle was measured using the midplane between the bilayer leaflets.

The employed values were $\kappa = 20$ kT, $\kappa_G = -16$ kT, $K_s = 50$ kT nm^{-2} and $\gamma = 3.6$ kT nm^{-1}. The bending modulus was obtained from refs 30,15, and 16 while the Gaussian modulus was obtained from refs 17, 20, and 19. The typical K_s value of 200 mJ/m^2 for phospholipids was obtained from micropipet experiments.[34,30] For the line tension, we employed 15 pN which is a midrange value of the experimental range 6.5−30 pN.[21,23,24]

When the membrane area remains constant (assumption valid for vesicles at zero tension) there is an analytical solution to the above equation:

$$\Delta G = 2\pi\gamma x - (2\kappa+\kappa_G)\frac{\pi x^2}{{R_0}^2} \quad (7)$$

If the nanoparticle is a sphere of radius r the pore has to open at least to this size ($x = r$) for release to be successful. Moreover, the radius of the vesicle wrapping the nanoparticle is just slightly larger by half of the membrane thickness t, so we can write $R_0 = r + {}^t/_2$.

The height of the free energy barrier associated with opening of the pore for the nanoparticle is

$$\Delta G = 2\pi\gamma R - (2\kappa+\kappa_G)\frac{\pi}{\left(1+\frac{t}{2r}\right)^2} \quad (8)$$

Therefore, larger nanoparticles experience higher free energy barrier for release, unless the radius is so small that the stable state of wrapping membrane is not a vesicle. The increase of the barrier height is roughly linear with the radius of the nanoparticle as $r \gg t$.

We can also calculate the expansion ratio χ of the nanoparticle radius that would provide enough energy to open a pore of size of the nanoparticle. The stretch energy from pore expansion is

$$\Delta G_{\text{stretch}} = \frac{1}{2}K_s\frac{(A-A_0)^2}{A_0} \quad (9)$$

$$= 2\pi K_s\frac{[(\chi r + t/2)^2 - (r+t/2)^2]^2}{(r+t/2)^2} \quad (10)$$

and the energy necessary to open a pore is given by eq 8. Using the above experimental values one obtains $\chi = 1.05$ for the nanoparticle of radius 5.0 nm and it is decreasing with increasing size of the nanoparticle. However, note that such nanoparticle expansion can lead to a kinetically trapped state (local free energy minimum), where the pore opened in the vesicle has a radius smaller than the nanoparticle (see Figure 5 between points b and c).

Release of spherocylinder. The cytosol release of a spherocylinder can be a spontaneous process if the ligand−receptor binding strength decreases below a threshold. We have estimated the threshold from the elastic model of a membrane for an ideal nondeformable spherocylinder. Upon release of the spherocylinder with radius R and length L the membrane bending energy will change as

$$\Delta E_B = 8\pi\kappa + \pi\kappa\frac{L}{R} - 8\pi\kappa = \pi\kappa\frac{L}{R} \quad (11)$$

and the loss of the attractive energy is

$$\Delta E_r = 2\pi\omega_r(2R^2 + RL) \quad (12)$$

where ω_r is residual attractive energy per area between spherocylinder and membrane. Therefore, release will be thermodynamically favorable when $\Delta E_B > \Delta E_r$. Leading to

$$\pi\kappa \frac{L}{R} > 2\pi\omega_r(2R^2 + RL) \quad (13)$$

$$\omega_r < \frac{L\kappa}{4R^3 + 2R^2L} \quad (14)$$

There are two limiting cases: first $L = \infty$ when $\omega_r = (\kappa/2R^2)$ and second $L = 0$ when spherocylinder becomes sphere and $\omega_r = 0$. This means that membrane prefers to be in a spherical geometry, and thus it should be easier to release the spherocylinder of any length.

This result is in contrast to the trend we have observed in our simulations, where a smaller residual ligand−receptor binding was necessary for release of a longer spherocylinder. The difference might be due to the kinetic effect as the membrane has to unwrap (lose all its attractive binding energy) first and then change its shape to spherical vesicle (gaining bending energy). Thus the transition barrier could be larger for longer spherocylinders.

Conflict of Interest: The authors declare no competing financial interest.

Acknowledgment. R.V. acknowledges support from Churchill College, Cambridge, the EU Seventh Framework Programm (Contract No. 286154—SYLICA project), and European Regional Development Fund (CZ.1.05/1.1.00/02.0068—Project CEITEC). D.F. and F.J.M.V. acknowledge ERC support (Advanced Grant Agreement 227758). D.F. acknowledges support from a grant of the Royal Society of London (Wolfson Merit Award).

REFERENCES AND NOTES

1. Davis, D. M.; Sowinski, S. Membrane Nanotubes: Dynamic Long-Distance Connections between Animal Cells. *Nat. Rev. Mol. Cell Biol.* **2008**, *9*, 431–436.
2. Yan, Y.; Such, G. K.; Johnston, A. P. R.; Best, J. P.; Caruso, F. Engineering Particles for Therapeutic Delivery: Prospects and Challenges. *ACS Nano* **2012**, *6*, 3663–3669.
3. Lammers, T.; Aime, S.; Hennink, W. E.; Storm, G.; Kiessling, F. Theranostic Nanomedicine. *Acc. Chem. Res.* **2011**, *44*, 1029–1038.
4. Martinez-Veracoechea, F. J.; Frenkel, D. Designing Super Selectivity in Multivalent Nano-particle Binding. *Proc. Natl. Acad. Sci. U.S.A.* **2011**, *108*, 10963–10968.
5. Carlson, C. B.; Mowery, P.; Owen, R. M.; Dykhuizen, E. C.; Kiessling, L. L. Selective Tumor Cell Targeting Using Low-Affinity, Multivalent Interactions. *ACS Chem. Biol.* **2007**, *2*, 119–127.
6. Vácha, R.; Martinez-Veracoechea, F. J.; Frenkel, D. Receptor-Mediated Endocytosis of Nanoparticles of Various Shapes. *Nano Lett.* **2011**, *11*, 5391–5395.
7. Reynwar, B. J.; Illya, G.; Harmandaris, V. a.; Muller, M. M.; Kremer, K.; Deserno, M. Aggregation and Vesiculation of Membrane Proteins by Curvature-Mediated Interactions. *Nature* **2007**, *447*, 461–464.
8. Le Bihan, O.; Bonnafous, P.; Marak, L.; Bickel, T.; Trépout, S.; Mornet, S.; De Haas, F.; Talbot, H.; Taveau, J.-C.; Lambert, O. Cryo-Electron Tomography of Nanoparticle Transmigration into Liposome. *J. Struct. Biol.* **2009**, *168*, 419–425.
9. Heidel, J. D.; Davis, M. E. Clinical Developments in Nanotechnology for Cancer Therapy. *Pharm. Res.* **2011**, *28*, 187–199.
10. Wagner, E. Polymers for siRNA Delivery: Inspired by Viruses to be Targeted, Dynamic, and Precise. *Acc. Chem. Res.* **2012**, *45*, 1005–1013.
11. Mukherjee, S.; Ghosh, R. N.; Maxfield, F. R. Endocytosis. *Physiol. Rev.* **1997**, *77*, 759–803.
12. Jones, D. S.; Silverman, A. P.; Cochran, J. R. Developing Therapeutic Proteins by Engineering Ligand-Receptor Interactions. *Trends Biotechnol.* **2008**, *26*, 498–505.
13. Cooke, I. R.; Deserno, M. Solvent-Free Model for Self-Assembling Fluid Bilayer Membranes: Stabilization of the Fluid Phase Based on Broad Attractive Tail Potentials. *J. Chem. Phys.* **2005**, *123*, 224710.
14. Helfrich, W. Possible Chromatographic Effect of Liquid-Crystalline Permeation. *Z. Naturforsch., A* **1973**, *28A*, 1968–1969.
15. Kucerka, N.; Tristram-Nagle, S.; Nagle, J. F. Structure of Fully Hydrated Fluid Phase Lipid Bilayers with Monounsaturated Chains. *J. Membr. Biol.* **2005**, *208*, 193–202.
16. Pan, J.; Tristram-Nagle, S.; Kucerka, N.; Nagle, J. F. Temperature Dependence of Structure, Bending Rigidity, and Bilayer Interactions of Dioleoylphosphatidylcholine Bilayers. *Biophys. J.* **2008**, *94*, 117–124.
17. Siegel, D. P.; Kozlov, M. M. The Gaussian Curvature Elastic Modulus of *N*-Monomethylated Dioleoylphosphatidylethanolamine: Relevance to Membrane Fusion and Lipid Phase Behavior. *Biophys. J.* **2004**, *87*, 366–374.
18. Brannigan, G.; Philips, P.; Brown, F. Flexible Lipid Bilayers in Implicit Solvent. *Phys. Rev. E* **2005**, *72*, 011915.
19. Deserno, M. Mesoscopic Membrane Physics: Concepts, Simulations, and Selected Applications. *Macromol. Rapid Commun.* **2009**, *30*, 752–771.
20. Siegel, D. P. The Gaussian Curvature Elastic Energy of Intermediates in Membrane Fusion. *Biophys. J.* **2008**, *95*, 5200–5215.
21. Taupin, C.; Dvolaitzky, M.; Sauterey, C. Osmotic Pressure-Induced Pores in Phospholipid Vesicles. *Biochemistry* **1975**, *14*, 4771–4775.
22. Evans, E.; Rawicz, W. Entropy-Driven Tension and Bending Elasticity in Condensed-Fluid Membranes. *Phys. Rev. Lett.* **1990**, *64*, 2094–2097.
23. Zhelev, D. V.; Needham, D. Tension-Stabilized Pores in Giant Vesicles: Determination of Pore Size and Pore Line Tension. *Biochim. Biophys. Acta Biomembr.* **1993**, *1147*, 89–104.
24. Karatekin, E.; Sandre, O.; Guitouni, H.; Borghi, N.; Puech, P.-H.; Brochard-Wyart, F. Cascades of Transient Pores in Giant Vesicles: Line Tension and Transport. *Biophys. J.* **2003**, *84*, 1734–1749.
25. Noguchi, H.; Gompper, G. Dynamics of Vesicle Self-Assembly and Dissolution. *J. Chem. Phys.* **2006**, *125*, 164908.
26. Speir, J. A.; Munshi, S.; Wang, G.; Baker, T. S.; Johnson, J. E. Structures of the Native and Swollen Forms of Cowpea Chlorotic Mottle Virus Determined by X-ray Crystallography and Cryo-Electron Microscopy. *Structure* **1995**, *3*, 63–78.
27. Larsson, D. S. D.; Liljas, L.; van der Spoel, D. Virus Capsid Dissolution Studied by Microsecond Molecular Dynamics Simulations. *PLoS Comput. Biol.* **2012**, *8*, e1002502.
28. Shinoda, W.; Nakamura, T.; Nielsen, S. O. Free Energy Analysis of Vesicle-to-Bicelle Transformation. *Soft Matter* **2011**, *7*, 9012–9020.
29. Needham, D.; Nunn, R. S. Elastic Deformation and Failure of Lipid Bilayer Membranes Containing Cholesterol. *Biophys. J.* **1990**, *58*, 997–1009.
30. Rawicz, W.; Olbrich, K. C.; McIntosh, T.; Needham, D.; Evans, E. Effect of Chain Length and Unsaturation on Elasticity of Lipid Bilayers. *Biophys. J.* **2000**, *79*, 328–339.
31. Cooke, I.; Kremer, K.; Deserno, M. Tunable Generic Model for Fluid Bilayer Membranes. *Phys. Rev. E* **2005**, *72*, 2–5.
32. Limbach, H.; Arnold, A.; Mann, B.; Holm, C. ESPResSo an Extensible Simulation Package for Research on Soft Matter Systems. *Comput. Phys. Commun.* **2006**, *174*, 704–727.
33. Bennett, C. Efficient Estimation of Free Energy Differences From Monte Carlo Data. *J. Comput. Phys.* **1976**, *268*, 245–268.
34. Evans, E.; Needham, D. Physical Properties of Surfactant Bilayer Membranes: Thermal Transitions, Elasticity, Rigidity, Cohesion and Colloidal Interactions. *J. Phys. Chem.* **1987**, *91*, 4219–4228.